# On the Observability of Robot Motion Under Active Camera Control

**Rajeev Sharma** **Seth Hutchinson**

The Beckman Institute, University of Illinois at Urbana-Champaign
405 N. Mathews Avenue, Urbana, IL 61801

## Abstract

*We define a measure of "observability" of robot motion that can be used in evaluating a hand/eye set-up with respect to the ease of achieving vision-based control. This extends the analysis of "manipulability" of a robotic mechanism in [9] to incorporate the effect of visual features. We discuss how the observability measure can be applied for active camera placement and for robot trajectory planning to improve the visual servo control. We use the examples of a planar 2-DOF arm and a PUMA-type 3-DOF arm to show the variation of the observability and manipulability measure with respect to the relative position of the active camera.*

## 1 Introduction

The integration of computer vision with robot motion control has steadily progressed, from early look and move systems in which vision was used to recognize and locate an object prior to its manipulation to current systems in which visual feedback is incorporated directly into the control feedback loop [1, 5, 8]. Vision helps in overcoming uncertainties in modeling the robot and its environment, thereby increasing the scope of robot applications to include tasks that were not possible without sensor feedback, for example welding [3]. At the same time, incorporation of visual feedback into the robot control raises many theoretical and practical questions that are unique to the use of computer vision. Resolving the issues involved lead to a variety of different approaches to the *visual servo control* or *robot hand/eye coordination* problem. In particular, an important distinction that can be made is that of the feedback representation mode, which can be either *position-based* or *image-based* [2, 8].

For visual servoing a set of image features are used to control the motion of the robot. Assuming that a set of appropriate image features are visible (and extracted using a suitable vision algorithm), the question that we are concerned with here is how will the features change with the motion of the robot. If a large motion of the robot produces very little change in the visual features then it may be difficult to use the differential change in the measured features to drive the robot. Hence we need some quantitative measure of the ability to observe changes in the image features with respect to differential motion of the robot.

Similar concern with respect to the differential change in the end-effector position (and orientation) relative to change in the joint configuration resulted in the definition of the term *manipulability* [9] or *dexterity* [4]. These measures, which depend on the particular robot mechanism and its posture, capture a sense of how far the robot is from a "singular" configuration. For robot control singular configurations are undesirable, since at those configurations the ability to move along one or more dimensions of the task space is lost. The manipulability measures are thus used in designing the robot mechanism and in determining the optimal configuration with respect to robot control. We extend these ideas to the situation when the camera is part of the hand/eye setup. The purpose of the "observability" measure is to quantify the goodness of a particular camera-manipulator juxtaposition. Such a measure can then be used to guide the placement of a camera, to plan the motion of an active camera for a given manipulator trajectory, or to plan the motion of the manipulator for a given camera position.

## 2 Basis of Visual Servo Control

As is standard in much of the robotics literature, we use $\mathbf{q}$ to represent the configuration of the robot. The space of all configurations of the robot (i.e. the configuration space) is represented by $\mathcal{C}$. We will assume that $\mathcal{C}$ is an $n$-dimensional space (which implies an $n$ degree-of-freedom robot). The task space of the robot, i.e. the set of positions and orientations that the robot tool can attain, will be denoted by $\mathcal{W} = \mathbf{R}^3 \times \mathrm{SO}(3)$. We will use $\mathbf{r} \in \mathcal{W}$ to denote an element of the task space. In the remainder of this section, we show how the robot's task space can be mapped to the camera's *visual feature space* and then we will consider the mapping from the robot's configuration space to the visual feature space.

If the robot is within the field of view of the cam-



1050-4729/94 $03.00 

era, then an image of the robot end-effector will be formed on the camera image plane. We assume that the projective geometry of the camera is modeled by perspective projection. We define the term ***visual feature*** to mean any real valued parameter that can be calculated from the projection of the robot on the camera image plane. Examples of visual features include the image plane coordinates of a point in the image, the area of a projected surface (e.g. the number of pixels in the projected surface), and the angle between projected edges. In general, a visual feature corresponds to the projection of some structural feature of the robot or to the relationship between the projections of multiple structural features of the robot. For example, the image plane coordinates of the projection of a vertex define two visual features. Likewise, the distance in the image plane between the projections of two vertices defines a visual feature (other examples are given in [8, 2]).

Prior to executing or planning visually controlled motions, the particular set of visual features that will be used must be chosen. A discussion of some of the issues related to feature selection can be found in [2]. Once we have chosen the set of $k$ visual features that will be used for control, we can define a visual feature vector $v = \langle v_1 \cdots v_k \rangle$. Since each $v_i$ is a (possibly bounded) real valued parameter, we have $v = \langle v_1 \cdots v_k \rangle \in \mathcal{V} \subseteq \Re^k$, where $\mathcal{V}$ represents the space of visual feature vectors. We will refer to $\mathcal{V}$ as the ***visual feature space.***

We represent the mapping from the position and orientation of the robot end-effector to the corresponding visual features by using the projective geometry of the camera by the function $\mathbf{v}$

$$\mathbf{v} : \mathcal{W} \rightarrow \mathcal{V}. \tag{1}$$

For example, if $\mathcal{V} \subseteq \Re^2$ is the space of $i, j$ image plane coordinates for the projection of the gripper tool center, then $\mathbf{v}(\mathbf{r}) = \langle x'_I(\mathbf{r}), x'_J(\mathbf{r}) \rangle$, where $x'_I(\mathbf{r})$ and $x'_J(\mathbf{r})$ are the coordinates of the projection of the tool center.

For visual servo control, it is necessary to relate differential changes in the visual features to differential changes in the position of the robot. The image Jacobian captures these relationships. In particular, the image Jacobian, $\mathbf{J}_v$ is a linear transformation from $\mathbf{T}_\mathbf{r}(\mathcal{W})$, the tangent space of $\mathcal{W}$ at $\mathbf{r}$, to $\mathbf{T}_\mathbf{v}(\mathcal{V})$, the tangent space of $\mathcal{V}$ at $\mathbf{v}$

$$\dot{\mathbf{v}} = \mathbf{J}_r \dot{\mathbf{r}}. \tag{2}$$

We will refer to $\dot{\mathbf{v}} \in \mathbf{T}_\mathbf{v}(\mathcal{V})$ as an visual feature velocity. The image Jacobian is given by

$$J_v(\mathbf{q}) = \left[\frac{\partial \mathbf{v}}{\partial \mathbf{r}}\right] = \begin{bmatrix} \frac{\partial v_1(\mathbf{r})}{\partial r_1} & \cdots & \frac{\partial v_1(\mathbf{r})}{\partial r_m} \\ \vdots & & \vdots \\ \frac{\partial v_k(\mathbf{r})}{\partial r_1} & \cdots & \frac{\partial v_k(\mathbf{r})}{\partial r_m} \end{bmatrix}. \tag{3}$$

By the implicit function theorem [7], if, in some neighborhood of $\mathbf{r}$, $m \leq k$ and $\text{rank}(\mathbf{J}_v) = m$, we can express the coordinates $v_{m+1} \ldots v_k$ as smooth functions of $v_1 \ldots v_m$. From this, we deduce that in order to track motion with $m$ degrees of freedom, $m < k$ implies that there are $k - m$ redundant visual features. Typically, this will result in a set of inconsistent equations (since the $k$ visual features will be obtained from a computer vision system, and therefore will likely be noisy). The implicit function theorem essentially gives us license to deal locally with the visual feature space in terms of an $m$-dimensional coordinate map by locally projecting $\mathcal{V}$ onto an $m$-dimensional subspace. Therefore, when $m \leq k$ and $\text{rank}(\mathbf{J}_v) = m$, we may apply the inverse function theorem to deduce that locally, an inverse $\mathbf{v}^{-1}$ exists, and is smooth.

Above, we have indicated that $\mathbf{J}_v$ is a function of the position of the moving object, $\mathbf{r}$, where $\mathbf{r}$ is given in camera coordinates. In the case where the camera is allowed to move, possibly an eye-in-hand system or an active vision system, it is convenient to express both the position of the object and the position of the camera with respect to some external fixed frame. In this case, we can reformulate the feature mapping and visual Jacobian as follows:

$$\mathbf{v} : \mathcal{C}_c \times \mathcal{W} \rightarrow \mathcal{V} \tag{4}$$

where $\mathcal{C}_c$ represents the configuration space of the camera. Often $\mathcal{C}_c$ will be defined in terms of the position of the lens center and the orientation of the image plane of the camera, expressed in terms of pan and tilt angles. In this case, we will explicitly represent the dependence of the visual feature values on camera parameters using the notation $\mathbf{v}(\mathbf{q}_c, \mathbf{r})$.

As can be seen from equation (2), the image space velocity is a linear combination of the columns of the image Jacobian. Therefore, if the rank of $\mathbf{J}_v$ drops below $m$, there will be certain visual feature velocities that are not possible, *i.e.* it is a singularity in the mapping from the task space to the visual feature space.

## 3 Observability of Robot Motion

As mentioned earlier, our goal in this paper is to present a quantitative value for the observability of an object's (possibly a robot manipulator) motion, given that the motion is determined by the observation of a set of visual features. We introduce such a measure, $w_v$ which is motivated by the manipulability measure first presented in [9], and

$$w_v = \sqrt{\det(\mathbf{J}_v \mathbf{J}_v^T)}. \tag{5}$$

We now study the physical meaning of the observability measure. Consider the set of all robot end-effector velocities $\dot{\mathbf{r}}$ such that

$$||\dot{\mathbf{r}}|| = (\dot{r}_1 + \dot{r}_2 + \ldots \dot{r}_m)^{1/2} \leq 1 \tag{6}$$

It can be shown that the corresponding set of visual feature velocities is given by the set of all $\dot{\mathbf{v}}$ such that

$$\dot{\mathbf{v}}^T (\mathbf{J}_v^+)^T \mathbf{J}_v \dot{\mathbf{v}} \leq 1, \tag{7}$$

where $JvP$ is an appropriate pseudoinverse of $\mathbf{J}_v$. Equation (7) defines a hyper-ellipsoid in the visual feature

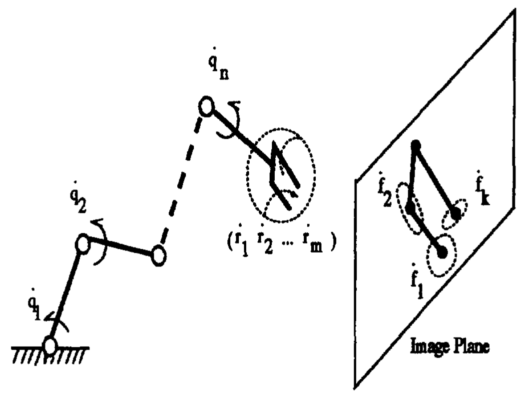


Figure 1: The observability ellipsoid in the visual feature space.

space (Fig. 1), which we shall refer to as the observability ellipsoid. The dimensions of the observability ellipsoid provide a quantitative evaluation of the observability of the robot motion given by $\dot{\mathbf{r}}$. The volume of the observability ellipsoid is given by $K\sqrt{\det(\mathbf{J}_v\mathbf{J}_v^T)}$, or $Kw_v$, where $K$ is a scaling constant that depends on the dimension of the ellipsoid. This volume provides a concise and intuitively pleasing measure of observability. Additional insights can be gained by examining the principal axes of the observability ellipsoid. Consider the singular value decomposition of $\mathbf{J}_v$

$$\mathbf{J}_v = \mathbf{U}\Sigma\mathbf{V}^T. \tag{8}$$

where

$$\mathbf{U} = [\mathbf{u}_1\mathbf{u}_2\ldots\mathbf{u}_k], \qquad \mathbf{V} = [\mathbf{v}_1\mathbf{v}_2\ldots\mathbf{v}_m] \tag{9}$$

are orthogonal matrices.

For $k < m$ we have

$$\Sigma = \left[\begin{array}{cccc|c} \sigma_1 & & & & \\ & \sigma_2 & & & \\ & & \cdot & & 0 \\ & & & \cdot & \\ & & & \sigma_k & \end{array}\right] \tag{10}$$

where $\Sigma \in \mathbf{R}^{k\times m}$ and the $\sigma_i$ are the singular values of $\mathbf{J}_v$, and $\sigma_1 \geq \sigma_2 \ldots \geq \sigma_k$.

For $m < k$ we have

$$\Sigma = \left[\begin{array}{cccc} \sigma_1 & & & \\ & \sigma_2 & & \\ & & \cdot & \\ & & & \cdot \\ & & & \sigma_m \\ \hline & & 0 & \end{array}\right] \tag{11}$$

It can be shown that the observability ellipsoid given by (7) has principal axes $\sigma_1\mathbf{u}_1, \sigma_2\mathbf{u}_2 \ldots \sigma_k\mathbf{u}_k$, and that the observability can be defined in terms of the singular values as

$$w_v = \sigma_1\sigma_2\cdots\sigma_s, \text{ with } \quad s = \min(k, m)$$

We now present several observations which are analogous to those given for manipulability in [9].

- In general, $w_v = 0$ holds if and only if $\text{rank}(\mathbf{J}_v) < m$, (i.e. for singularities in $\mathbf{v}$).
- When $k = m$ (i.e. when there are no redundant features) $w_v = |\det(\mathbf{J}_v)|$.
- Suppose that there is some error in the measured visual feature velocity, $\Delta\dot{\mathbf{v}}$. We can bound the corresponding error in the computed object velocity, $\Delta\dot{\mathbf{r}}$, by

$$(\sigma_1)^{-1} \leq \frac{||\Delta\dot{\mathbf{r}}||}{||\Delta\dot{\mathbf{v}}||} \leq (\sigma_k)^{-1}. \tag{12}$$

## 4 Optimization of Active Camera Position

We briefly formalize the problem of optimal camera placement with respect to our measure of observability $w_v$. We only address issues related to observability of motion, and do not address issues related to other criteria, e.g. occlusion, field of view, depth of field, focus, etc.. These issues have been addressed in [6]. In fact, the methods presented in [6] produce a set of constraints on camera position and orientation. These can be used as additional constraints in the optimization process discussed here.

We will address two problems: (1) optimal camera placement for a fixed camera system that is used to control a robot performing some predetermined motion, e.g. a robot grasping an object, and (2) planning an optimal camera trajectory for use by an eye-in-hand system, e.g. an eye-in-hand system monitoring a second robot performing a task.

In order to perform the optimization, we posit the following cost functional:

$$\text{cost}(\mathbf{q}_c) = -\int (w_v(\mathbf{r}, \mathbf{q}_c))dt \tag{13}$$

where $\mathbf{q}_c$ is a vector of camera parameters that determines the camera position and orientation, $\mathbf{r}(t)$ is the parameterized trajectory followed by the robot end-effector, and the integral is taken over the duration of a given trajectory. With this formulation, the problem of optimal camera placement reduces to finding $\mathbf{q}_c^*$ such that

$$\text{cost}(\mathbf{q}_c^*) = \min_{\mathbf{q}_c \in \mathcal{C}_c} -\int (w_v(\mathbf{r}, \mathbf{q}_c))dt. \tag{14}$$

When other viewpoint constraints are taken into account, such as those given in [6], $\mathcal{C}_c$ would be restricted to the set of valid camera configurations.

For an eye-in-hand system, the problem is more difficult. In this case, we must choose a camera trajectory, $\mathbf{q}_c^*(t)$, such that

$$\text{cost}(\mathbf{q}_c^*(\cdot)) = \min_{\mathbf{q}_c(\cdot)} -\int (w_v(\mathbf{r}, \mathbf{q}_c))dt. \tag{15}$$

These formulations represent very difficult optimization problems. Therefore, it may be more expedient to proceed with a simplified analysis. For example, for a fixed camera, we might choose to use

$$\mathrm{cost}_a(\mathbf{q}_c^*) = \min_{\mathbf{q}_c \in \mathcal{C}_c} \max_t(-w_v(\mathbf{r}, \mathbf{q}_c)). \quad (16)$$

In general, this class of problems can only be solved by placing strict limitations on the class of trajectories that are permitted for the active camera.

## 5 Combining Observability & Manipulability

The system designer is often free to choose where in the robot workspace a particular task is to be performed. In such cases, it is desirable to choose the robot trajectory and the camera location so that both observability and manipulability are optimized. Manipulability was first introduced in [9], and is defined as

$$w_r = \sqrt{\det(\mathbf{J}_r \mathbf{J}_r^T)} \quad (17)$$

where $\mathbf{J}_r$ is the manipulator Jacobian matrix, and

$$\dot{\mathbf{r}} = \mathbf{J}_r \dot{\mathbf{q}} \quad (18)$$

is the expression relating the robot joint velocities, $\dot{\mathbf{q}}$, to the velocity of the end effector, $\dot{\mathbf{r}}$.

Combining (18) and (2) we obtain

$$\dot{\mathbf{v}} = \mathbf{J}_v \mathbf{J}_r \dot{\mathbf{q}} \quad (19)$$

Let $\mathbf{J}_c = \mathbf{J}_v \mathbf{J}_r$ denote the composite Jacobian matrix. We now define a measure, $w_c$, which combines the effect of manipulability and observability, and is given by

$$w_c = \sqrt{\det(\mathbf{J}_c \mathbf{J}_c^T)}. \quad (20)$$

We note that, in general, $w_c \neq w_v w_r$, except in the special non-redundant case when $n = m = k$. The equality ($w_c = w_v w_r$), in fact, is achieved in this case because both the manipulator Jacobian $\mathbf{J}_r$ and the image Jacobian $\mathbf{J}_v$ are square matrices.

The composite Jacobian $\mathbf{J}_c$ relates differential changes in joint positions of the robot to differential changes in the observed visual features. In particular, consider the set of all joint velocities $\dot{\mathbf{q}}$ such that

$$||\dot{\mathbf{q}}|| = (\dot{q}_1 + \dot{q}_2 + \ldots \dot{q}_n)^{1/2} \leq 1. \quad (21)$$

It can be shown that the corresponding set of visual feature velocities is given by the set of all $\dot{\mathbf{v}}$ such that

$$\dot{\mathbf{v}}^T (\mathbf{J}_c^+)^T \mathbf{J}_c \dot{\mathbf{v}} \leq 1, \quad (22)$$

where $\mathbf{J}_c^+$ is an appropriate pseudoinverse of $\mathbf{J}_c$.

Thus, we once again obtain an observability ellipsoid, but in this case, the dimensions of the observability ellipsoid provide a quantitative evaluation of the observability of the joint motion given by $\dot{\mathbf{q}}$.

A second approach to the the simultaneous optimization of observability and manipulability is to formulate a cost functional that allows us to independently consider observability and manipulability. We can modify the cost function given in (13) to include manipulability,

$$\mathrm{cost}(\mathbf{r}, \mathbf{q}_c) = -\int [k_v(w_v(\mathbf{r}, \mathbf{q}_c)) + k_r(w_r(\mathbf{r}))]dt \quad (23)$$

where $k_v$ and $k_r$ are constants that allow us to weight the relative importance of observability and manipulability. The advantage to this formulation is that it allows us to decouple the tasks of robot trajectory planning and camera trajectory planning.

## 6 2-DOF Planar Arm

We consider a two-link planar arm (Fig. 2), where the task space can be described by $P(X, Y)$, a point on the robot's end-effector and the joint space is described by $(\theta_1, \theta_2)$. The camera position is described by the spherical coordinates $(R, \theta, \phi)$ while the orientation of the camera is fixed such that its optical axis is maintained parallel to the $Z$ axis. Now, for visual servo control of the 2-DOF planar robot, two image parameters would be sufficient, as described earlier. We consider the image of the point $P$, given by $(u, v)$ to be the feature to be tracked and used for visual control. For this situation we will analyze how the manipulability and observability vary for different positions of the active camera and the trajectory of the camera. We use the notation introduced earlier and omit the details of the derivation for brevity.

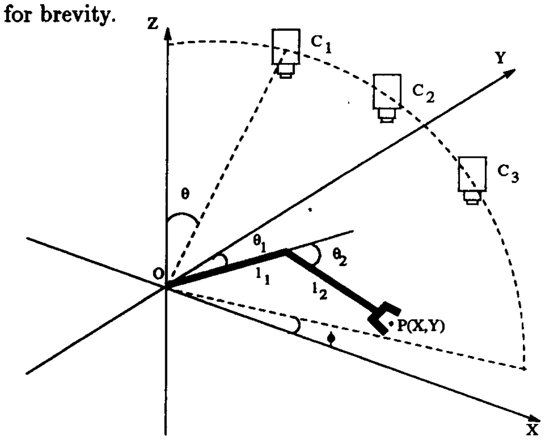


Figure 2: The relative position of the camera and the 2-DOF Planar Arm

$$\mathbf{J}_r = \begin{bmatrix} l_1 \cos\theta_1 + l_2\cos(\theta_1+\theta_2) & l_2\cos(\theta_1+\theta_2) \\ -l_1\sin\theta_1 - l_2\sin(\theta_1+\theta_2) & -l_2\sin(\theta_1+\theta_2) \end{bmatrix}$$

The manipulability, $w_r = |det(\mathbf{J}_r)| = l_1 l_2 |\sin\theta_2|$

$$\mathbf{J}_v = \begin{bmatrix} \frac{-f}{R\cos\theta} & 0 \\ 0 & \frac{-f}{R\cos\theta} \end{bmatrix}$$

The Observability, $w_v = |det(\mathbf{J}_v)| = \frac{f^2}{R^2\cos^2\theta}$

For this example we consider only the non-redundant case where both $\mathbf{J}_v$ and $\mathbf{J}_r$ are square matrices, thus we simplify Equation 20 to combine the observability and manipulability, giving

$$w_c = w_v . w_r = \frac{f^2 l_1 l_2 |\sin\theta_2|}{R^2\cos^2\theta}$$

Fig. 3 shows the variation of $w_c$ with the two camera parameters $R$ (varied from 30 to 40 unit distance) and $\theta$

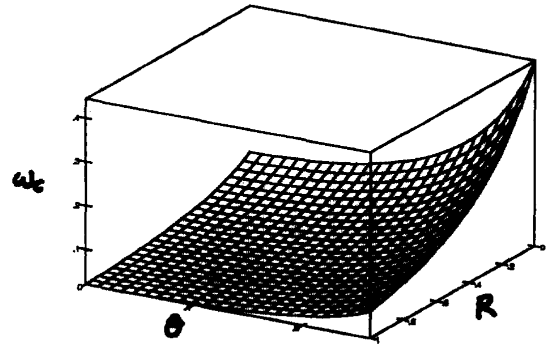

Figure 3: Variation of $w_c$ with different camera positions (planar robot).

(varied from 0 to $\pi/3$, for a particular pose of the robot ($\theta_2 = \pi/2$; $l_1 = l_2 = 10$; $f = 1$). In this simple case we can see that observability would increase as either $R$ or $\theta$ decreases. A singular position is reached when the $\theta = \pi/2$, or the the axis of the camera lies on the $X - Y$ plane.

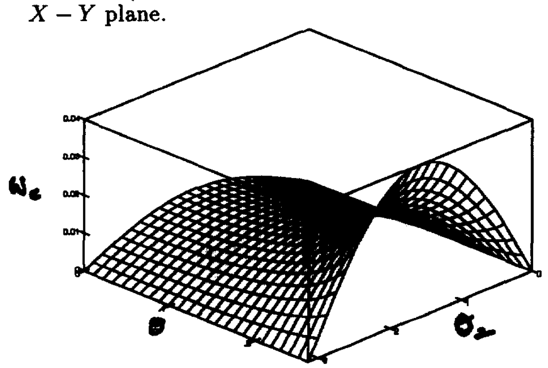

Figure 4: Variation of $w_c$ for a given camera and robot trajectory (planar robot).

Fig. 4 shows the variation of the combined manipulability and observability measure $w_c$ against a variation of the camera parameter $\theta$ (from 0 to $\pi/3$, with fixed $R$ = 100) and a circular trajectory of the end effector of the robot as traced by changing $\theta_2$ (from 0 to $\pi$), with $\theta_1$ fixed. As discussed in the previous section, an effective trajectory planning strategy using a cost function that uses $w_c$ would be one along the maxima of surface in Fig. 4.

## 7 3-DOF PUMA-type Arm

In this section we consider a Puma-type robot with three degrees of freedom (Fig. 5). The task space is described by $P(X, Y, Z)$, the position of a point in the end effector, while the joint space is described by $(\theta_1, \theta_2, \theta_3)$ the three joint angles. Unlike the previous case here we consider a more complicated motion of the cam-

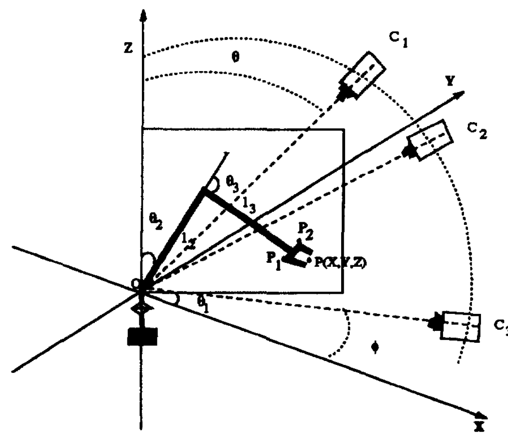

Figure 5: The relative position of the camera and Puma 3-DOF Arm

era, where its orientation changes but the optical axis passes through the origin of the common coordinate system, as shown in Fig. 5. This constraint on the camera helps us to describe its motion with the help of only three parameters–the spherical coordinates of its position $(R, \theta, \phi)$ even though the actual orientation of the camera is also changed. For achieving the necessary servo control we need to track three image features. We consider two points on its end effector ($P_1$ and $P_2$ of Fig. 5), and describe the feature space in terms of the $x$ and $y$ image coordinates of the first point and the $x$ coordinates of the second point.

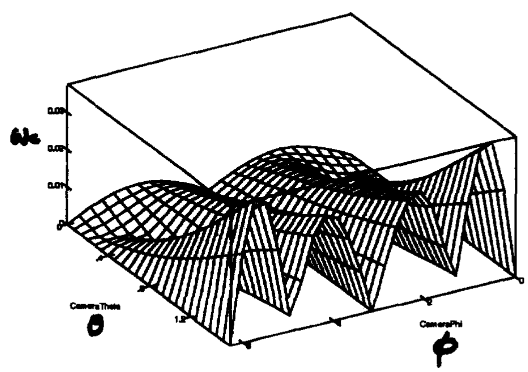

Figure 6: Variation of $w_c$ with different camera positions (puma robot).

To compute the manipulability and observability measures, we first compute the manipulator Jacobian $\mathbf{J}_r$ and the image Jacobian $\mathbf{J}_v$ and then compute their determinants to compute $w_c$ by a simple product because both $\mathbf{J}_r$ and $\mathbf{J}_v$ are square matrices. We omit the details of the derivation due to lack of space. Instead we show the plot of the variation of $w_c$ with parameterized variation of the camera postion in Fig. 6 with a fixed pose of the robot. Next we plot the variation of $w_c$ with both the position of the camera ($\theta$) while the robot end effector traces a trajectory defined by a parameterize change of all three robot joint angles from 0 to $\pi$ in equal increments. A study of the variation shows clearly the influence of the relative position of the camera and the robot end effector. It would also serve to motivate the effectiveness of the measure of observability (along with manipulability) to steer the robot away from singularities, and perhaps even use the measure as part of trajectory optimization. This would ensure the best use of the observability within the constraints of a given task.

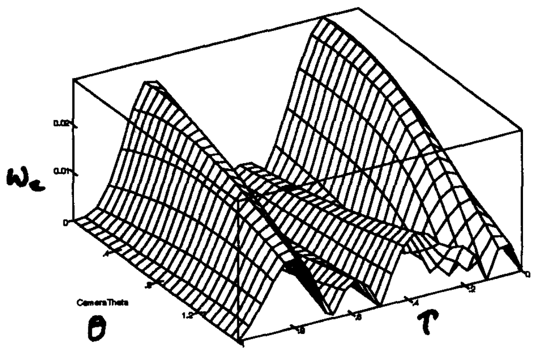

Figure 7: Variation of $w_c$ for a given camera and robot trajectory (puma robot).

## 8 Discussion and Conclusions

Observability represents a single scalar measure corresponding to the volume of the observability ellipsoid at a particular configuration. Thus it can only capture certain aspect of the ease of visual control. [4] gives a very good discussion of the physical meaning and shortcomings of the various dexterity measures which can be applied to the observability measure presented in this paper as well.

The measure of observability relates only a local property of the hand/eye setup which is important for visual servo control. However, if the same camera is to be used for other aspects of the task, for example, exploring [6] and task monitoring [10] then global optimization problems analogous to the ones posed in sections 4 and 5 would need to be solved. The optimization over an entire task may be hard to achieve thus should motivate approximate techniques that give the most importance to the critical parameters in determining the camera position at a given time.

Despite its shortcomings, the measure of observability that we introduce captures a very basic property of relative camera position in a hand/eye setup. It has a very intuitive meaning and helps to provide a formal basis for positioning a camera relative to a robot, in controlling an active camera, and in trajectory planning of the robot. It would enable one to achieve the optimal way of capturing the changes in the features for a given change in the robot position thus improving visual servo control. The examples presented in the paper should help in explaining the utility of the measure. Besides the applications discussed, the observability could also be used for selecting the set of image features from a candidate set for actually controlling the robot. Further research is needed to show how the measure can actually be incorporated in the robot/camera trajectory planning to give tractable results. But the results in this paper should provide an important step toward realizing the full potential of having an *active* camera for visual servo control.

## References


[1] P. Allen, B. Yoshimi, and A. Timcenko. Real-time Visual Servoing. In *Proc. DARPA Image Understanding Workshop*, pages 909–918, 1990.

[2] J. T. Feddema, C. S. George Lee, and O. R. Mitchell. Weighted Selection of Image Features for Resolved Rate Visual Feedback Control. *IEEE Transactions on Robotics and Automation*, 7:31–47, 1991.

[3] P. K. Khosla, C. P. Neuman, and F. B. Prinz. An Algorithm for Seam Tracking Applications. *International Journal of Robotics Research*, 4(1):27–41, 1985.

[4] J-O. Kim and P. K. Khosla. Dexterity Measures for Design and Control of Manipulators. In *Proc. IEEE/RSJ Int. Workshop on Intelligent Robots and Systems*, pages 758–763, 1991.

[5] S. B. Skaar, W. H. Brockman, and R. Hanson. Camera-Space Manipulation. *International Journal of Robotics Research*, 6(4):20–32, 1987.

[6] K. Tarabanis and R. Y. Tsai. Sensor Planning for Robotic Vision: A Review. In O. Khatib, J. J. Craig, and T. Lozano-Pérez, editors, *Robotics Review 2*. MIT Press, Cambridge, MA, 1992.

[7] F. W. Warner. *Foundations of Differentiable Manifolds and Lie Groups.* Springer-Verlag, New York, 1983.

[8] L. E. Weiss, A. C. Sanderson, and C. P. Neuman. Dynamic Sensor-Based Control of Robots with Visual Feedback. *IEEE Journal of Robotics and Automation*, 3:404–417, 1987.

[9] T. Yoshikawa. Analysis and Control of Robot Manipulators with Redundancy. In *Robotics Research: The First Int. Symposium*, pages 735–747. MIT Press, 1983.

[10] J. Y. Zheng, Q. Chen, and A. Tsuji. Active Camera Guided Manipulation. In *Proc. IEEE International Conference on Robotics and Automation*, pages 632–638, 1991.